

10. A. M. Kalsin *et al.*, *Science* **312**, 420–424 (2006).
11. S. Y. Park *et al.*, *Nature* **451**, 553–556 (2008).
12. D. Nykypanchuk, M. M. Maye, D. van der Lelie, O. Gang, *Nature* **451**, 549–552 (2008).
13. Q. Chen, S. C. Bae, S. Granick, *Nature* **469**, 381–384 (2011).
14. Y. Wang *et al.*, *Nature* **491**, 51–55 (2012).
15. X. Ye *et al.*, *Nat. Chem.* **5**, 466–473 (2013).
16. Materials and methods are available as supplementary materials on Science Online.
17. J. J. Choi *et al.*, *J. Am. Chem. Soc.* **133**, 3131–3138 (2011).
18. C. Zeng, C. Liu, Y. Chen, N. L. Rosi, R. Jin, *J. Am. Chem. Soc.* **138**, 8710–8713 (2016).
19. G. A. DeVries *et al.*, *Science* **315**, 358–361 (2007).
20. C. A. Hunter, J. K. M. Sanders, *J. Am. Chem. Soc.* **112**, 5525–5534 (1990).
21. M. Nishio, *Phys. Chem. Chem. Phys.* **13**, 13873–13900 (2011).
22. R. J. Macfarlane *et al.*, *Science* **334**, 204–208 (2011).
23. W. D. Luedtke, U. Landman, *J. Phys. Chem.* **100**, 13323–13329 (1996).
24. R. L. Whetten *et al.*, *Acc. Chem. Res.* **32**, 397–406 (1999).
25. P. W. Anderson, *Science* **177**, 393–396 (1972).
26. Q.-F. Sun *et al.*, *Science* **328**, 1144–1147 (2010).
27. C. L. Cleveland, U. Landman, *J. Chem. Phys.* **94**, 7376 (1991).
28. P. D. Jadzinsky, G. Calero, C. J. Ackerson, D. A. Bushnell, R. D. Kornberg, *Science* **318**, 430–433 (2007).
29. Y. Chen *et al.*, *J. Am. Chem. Soc.* **137**, 10076–10079 (2015).
30. C. Zeng *et al.*, *Sci. Adv.* **1**, e1500045 (2015).

## ACKNOWLEDGMENTS

R.J. thanks the Air Force Office of Scientific Research [award no. FA9550-15-1-9999 (FA9550-15-1-0154)] and the Camille

Dreyfus Teacher-Scholar Awards Program for financial support. All data are available in the main text and in the supplementary materials. The x-ray crystallographic coordinates have been deposited in Cambridge Crystallographic Data Centre with CCDC number 1511348.

## SUPPLEMENTARY MATERIALS

www.sciencemag.org/content/354/6319/1580/suppl/DC1  
Materials and Methods  
Supplementary Text  
Figs. S1 to S11  
Tables S1 and S2

22 September 2016; accepted 16 November 2016  
10.1126/science.aak9750

## MIGRATION

# Mass seasonal bioflows of high-flying insect migrants

Gao Hu,<sup>1,2,3\*</sup> Ka S. Lim,<sup>2</sup> Nir Horvitz,<sup>4</sup> Suzanne J. Clark,<sup>2</sup> Don R. Reynolds,<sup>5</sup> Nir Sapir,<sup>6</sup> Jason W. Chapman<sup>2,3\*</sup>

Migrating animals have an impact on ecosystems directly via influxes of predators, prey, and competitors and indirectly by vectoring nutrients, energy, and pathogens. Although linkages between vertebrate movements and ecosystem processes have been established, the effects of mass insect “bioflows” have not been described. We quantified biomass flux over the southern United Kingdom for high-flying (>150 meters) insects and show that ~3.5 trillion insects (3200 tons of biomass) migrate above the region annually. These flows are not randomly directed in insects larger than 10 milligrams, which exploit seasonally beneficial tailwinds. Large seasonal differences in the southward versus northward transfer of biomass occur in some years, although flows were balanced over the 10-year period. Our long-term study reveals a major transport process with implications for ecosystem services, processes, and biogeochemistry.

Latitudinal migrations of vast numbers of flying insects, birds, and bats (1–7) lead to huge seasonal exchanges of biomass and nutrients across the Earth’s surface (8–11). Because many migrant species (particularly insects) are extremely abundant (1, 5), seasonal migrations may profoundly affect communities through predation and competition while transferring enormous quantities of energy, nutrients, propagules, pathogens, and parasites between regions, with substantial effects on essential ecosystem services, processes, and biogeochemistry (8–11), and, ultimately, ecosystem function.

Latitudinal bird migrations are well characterized; for example, 2.1 billion passerines migrate annually between Europe and Africa (2), integrating multisensory navigational information (12), exploiting favorable winds and adopting adaptive

flight behaviors (13). By comparison, even though insect migration surpasses all other aerial migratory phenomena in terms of sheer abundance (1), latitudinal insect migration is largely unquantified, in particular for the majority of species that migrate hundreds of meters above the ground (5). Specialized radar techniques are required to study these high-flying insect migrants, as they are too small to carry transmitters or to be observed by any other means (14). Until now, radar studies have been aimed almost exclusively at quantifying migrations of relatively few nocturnal species of agricultural pests (3).

We quantified annual abundance and biomass of three size categories of diurnal and nocturnal insects migrating above an area of ~70,000 km<sup>2</sup> of the southern United Kingdom (Fig. 1A), between 150 and 1200 m above ground level (agl) (Fig. 1B), from 2000 to 2009 (15). Abundance and biomass values for medium (10 to 70 mg) and large insects (70 to 500 mg) (referred to collectively as “larger insects”) were calculated from measurements of >1.8 million individuals (table S1) detected by vertical-looking entomological radars (VLRs) located in the southern United Kingdom (Fig. 1A). The VLRs provide a range of information—including body mass, flight altitude, aerial density, displacement speed, displacement direction, and flight heading—for all individual

insects of >10-mg body mass that fly through the vertically pointing beam within the altitude range of 150 to 1200 m agl (14). Annual abundance and biomass values for larger insects migrating over the study area were extrapolated from the aerial densities and body masses recorded above the VLR locations (15). The third size category, small insects (<10 mg), are not sampled by VLRs, and so abundance and biomass data were calculated from aerial netting samples (16) taken ~200 m agl near one of the radars (Fig. 1A) and extrapolated to the study area (15). Larger diurnal migrants are predominantly beneficial species, including hoverflies, ladybeetles, carabid beetles, and butterflies (14–17), and the most abundant small day-fliers are cereal aphids (16). The commonest larger nocturnal insects are lacewings and noctuid moths (14, 16), whereas Diptera constitute the majority of the small nocturnal insects (16).

An annual mean of 3.37 trillion insects (range 1.92 to 5.01 × 10<sup>12</sup>) (Fig. 1C and table S2) migrated high above the study region, comprising 3200 tons of biomass (fig. S1 and table S3), and >70% of that biomass was from migration that occurred during daytime (Fig. 1C and table S2). Numerically, >99% of individuals were small insects; although the 15 billion medium and 1.5 billion large insects made up only 0.4% and 0.05% of the annual abundance (table S2), they accounted for a substantial proportion of the biomass: 12% (380 tons) and 7% (225 tons), respectively (table S3).

By analyzing 1320 daytime “mass migrations” (15) involving 1.25 million VLR-detected insects and 898 nocturnal mass migrations involving 126,000 insects (table S1), we characterized migration directions of the larger insects during “spring” (May to June), “summer” (July) and “fall” (August to September) (fig. S2 and table S4). Although high-altitude winds blew consistently toward the northeast or east in all three seasons (Rayleigh tests; daytime: spring, 60°; summer, 66°; fall, 84°; nighttime: spring, 69°; summer, 81°; fall, 101°) (Fig. 2A and table S5), mass migrations of larger insects did not simply move with the prevailing southwesterly winds. During the spring, mass migrations were consistently toward the north (Rayleigh tests; daytime: medium, 333°; large, 329°; nighttime: medium, 349°; large, 349°) (Fig. 2A), and this indicates that migration occurred on winds with a significantly more southerly component than prevailing winds (Watson-Wheeler tests; *P* < 0.0001 in all cases) (table S5).

<sup>1</sup>College of Plant Protection, Nanjing Agricultural University, Nanjing, China. <sup>2</sup>Rothamsted Research, Harpenden, Hertfordshire, UK. <sup>3</sup>Centre for Ecology and Conservation, and Environment and Sustainability Institute, University of Exeter, Penryn, Cornwall, UK. <sup>4</sup>Movement Ecology Laboratory, Department of Ecology, Evolution, and Behavior, The Hebrew University, Jerusalem, Israel. <sup>5</sup>Natural Resources Institute, University of Greenwich, Chatham, Kent, UK. <sup>6</sup>Animal Flight Laboratory, Department of Evolutionary and Environmental Biology, University of Haifa, Haifa, Israel.

\*Corresponding author. Email: hugao@njau.edu.cn (G.H.); j.chapman2@exeter.ac.uk (J.W.C.)

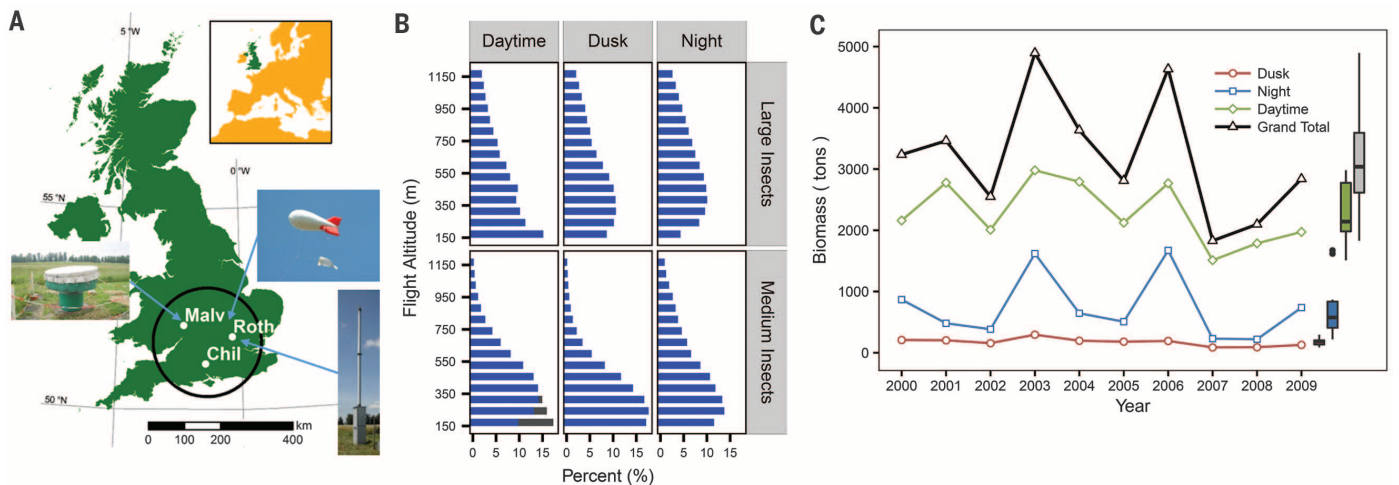


**Fig. 1. Monitoring migration intensity above the southern United Kingdom.** (A) The intensity and direction of high-altitude insect migration through the atmosphere 150 to 1200 m above ground level (agl) was measured over a 70,000-km<sup>2</sup> region of the southern United Kingdom (black circle) under continual surveillance from vertical-looking radars (VLR, left inset) at three locations (white dots); the aerial insect fauna were sampled by balloon-supported aerial netting at 200 m agl (center-right inset) and 12-m-high

suction traps (bottom-right inset). (B) Vertical profiles of larger insect (>10 mg) migration intensity over the sampling range of the VLRS. (C) Annual totals of insects migrating above the study region, during daytime, dusk, and night, as well as combined for the whole 24 hours. Lines represent annual totals; in the box plots, the central bar represents the median, boxes represent the interquartile range (IQR), whiskers extend to observations within  $\pm 1.5$  times the IQR and dots represent outliers.

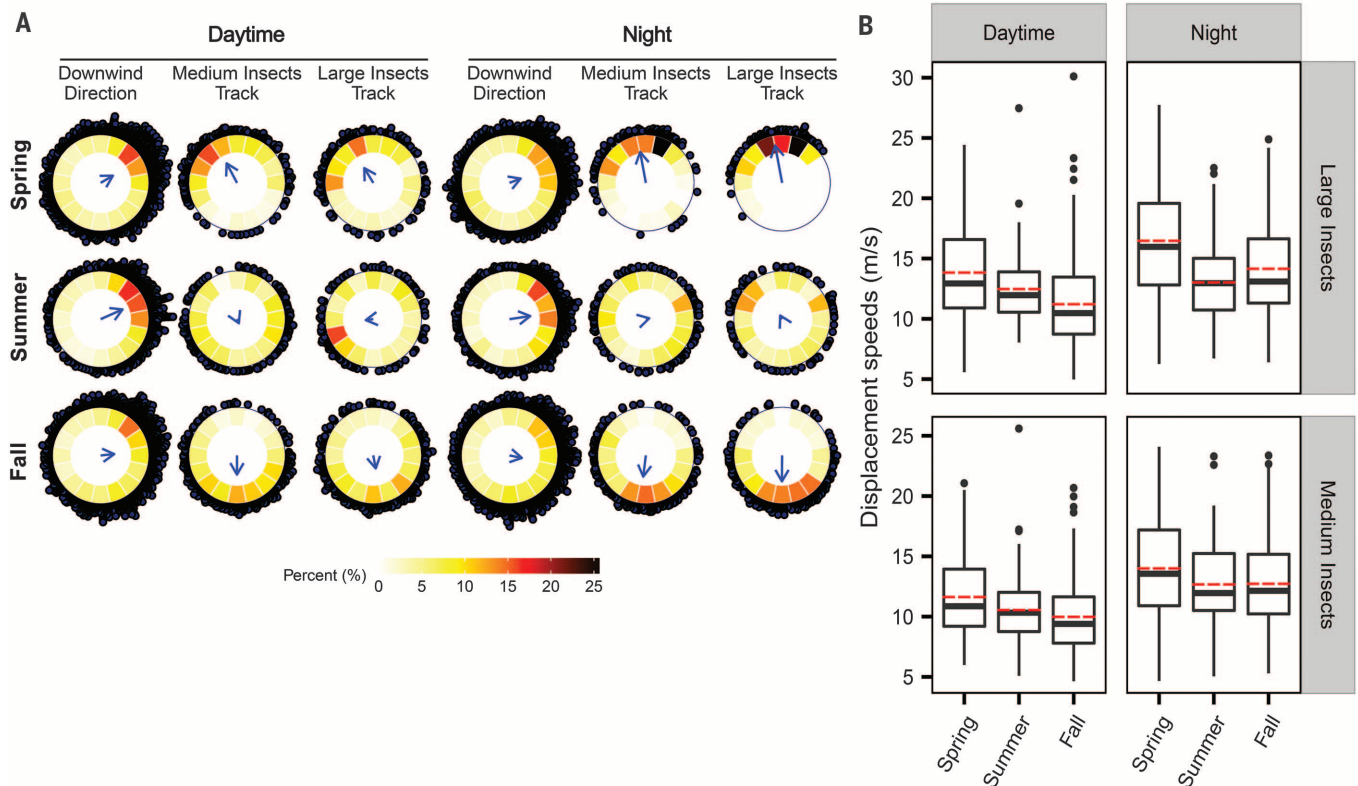


**Fig. 2. Migratory directions and speeds of high-flying larger insects.** (A) Despite prevailing winds blowing toward the northeast in all seasons, migratory tracks and headings occurred predominantly in seasonally beneficial directions in spring and fall but were randomly directed in summer. Small black circles on the periphery of the circular histograms represent mean directions of individual mass migrations, and the color bar indicates the percentage of migrations in

each 22.5° bin. The bearing of the blue arrow indicates the overall mean direction, and arrow length represents the circular resultant length ( $r$ ). (B) Migrants achieved fast displacement speeds. Solid black bars represent medians, dashed red lines represent means, boxes represent the IQR, whiskers extend to observations within  $\pm 1.5$  times the IQR, and dots represent outliers.

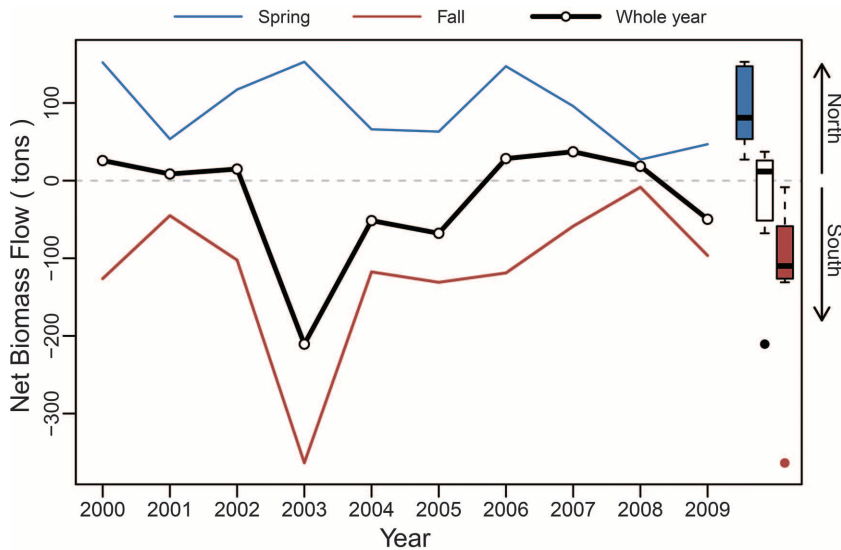


**Fig. 3. Annual patterns of net directional migration.** The net flow of biomass of larger insects above the study region, in spring, fall, and the whole year. Negative values indicate a net southward movement; positive values indicate a net northward movement. In the box plots, central bars represent median values, boxes represent the IQR, whiskers extend to observations within  $\pm 1.5$  times the IQR, and dots represent outliers.

Summer mass migrations were randomly directed (Rayleigh tests;  $P > 0.05$  in all cases) (Fig. 2A and table S5), this indicated an absence of wind selectivity. By contrast, fall mass migrations were consistently directed toward the south (Rayleigh tests; daytime: medium,  $174^\circ$ ; large,  $159^\circ$ ; nighttime: medium,  $181^\circ$ ; large,  $180^\circ$ ) (Fig. 2A), and this indicates active selection of winds with a significantly more northerly component than the prevailing winds (Watson-Wheeler tests;  $P < 0.0001$  in all cases) (table S5). These relationships indicate preferred movement directions during the spring and fall, as well as selection of days and nights with favorably directed tailwinds. Seasonally beneficial migration directions have been previously reported in a few species of large insects, notably pest noctuid moths (3, 14, 18), but our findings demonstrate the ubiquity of such movements among a diverse array of insect migrants. Because small insects fall below the VLR's detection threshold (14) and, thus, their tracks cannot be directly measured, we used aphid migration intensity as representative of all small insect migration (fig. S3) by analyzing wind directions associated with mass migrations of aphids (15). We found that aphid migration directions closely match prevailing wind directions, i.e., toward the northeast in all seasons (fig. S4), and, therefore, conclude that these small insects do not have mechanisms for selecting seasonally beneficial winds.

The greatest amount of variation in the aerial density of diurnal migrants was explained by surface meteorological conditions associated with fine weather (table S6): Migration intensity was greatest on warm days (fig. S5A) with moderate to high surface heat flux (fig. S5B) and low surface wind speeds (fig. S5C). However, the strong relationship with fine weather does not explain the directed movements of the larger insects in spring and fall. Models indicated that during

these seasons (but not summer), surface wind direction was also correlated with migration intensity, with high densities associated with southerly winds in the spring and northerly winds in the fall (table S6). Surface and high-altitude daytime wind directions were strongly correlated in all seasons (tests for T-linear association;  $P < 0.001$  in all cases) (fig. S6) but not at night (18). Thus, surface wind direction provides a reliable cue regarding the suitability of winds aloft for diurnal migrants at take-off but not for nocturnal migrants, which must use other methods for assessing high-altitude wind direction (19). The ubiquity of tailwind selectivity in such a diverse group indicates that compass mechanisms must be universal in larger insect migrants.

If high-flying insects have a compass sense, one would predict that, in addition to selecting a favorable tailwind, they would also orientate in the seasonally beneficial direction and, thus, actively contribute to their wind-assisted displacement. Such "common orientation" was indeed highly prevalent in the larger insects (table S1), and headings were close to tracks (fig. S7): northward in the spring and southward in the fall (table S7). The close correspondence between headings and tracks signifies that larger insects added much of their self-powered airspeed to the wind vector and thus achieved rapid displacement speeds [10 to 16 m/s ( $36$  to  $58$  km hr $^{-1}$ )] (Fig. 2B and table S7). A flight duration of 4 hours could therefore result in transport over  $>200$  km, and during spring and fall, this transfer of biomass and nutrients occurs in predictable directions.

What are the implications of this high-altitude insect movement? Insect bodies are typically composed of 10% nitrogen and 1% phosphorus by dry weight (20), and as such, they represent a rich source of nutrients that can be limiting for plant productivity (17). The 3200 tons of biomass

moving annually above our study region contains  $\sim 100,000$  kg of N and 10,000 kg of P, representing 0.2% of the surface deposits of N and 0.6 to 4.7% of P from the atmosphere, and making up  $5.78 \times 10^{12}$  Joules of energy (15). To put these seasonal movements in context, the annual airborne insect biomass  $>150$  m above the southern United Kingdom is 4.5 times the 2.2 billion (700 tons) of bogong moths (*Agrotis infusa*) that migrate to the Australian Alps every summer (7, 9), 7.7 times the 30 million songbird migrants (415 tons) that depart the United Kingdom for Africa each fall (table S8), and  $>40$  times the 150 million monarch butterflies (75 tons) that migrate between eastern North America and Mexico (14).

If the spring and fall movements documented here perfectly counterbalance each other, there would be no net annual exchange of energy and nutrients, and the principal consequences would be the exchange of genes, pathogens, and parasites. Over the 10-year study, we found that net northward spring movements of larger insects were almost exactly cancelled out by net southward fall movements; however, on an annual basis, the net flux could be up to 200 tons greater in either direction (Fig. 3). Such insect movements represent an underappreciated mechanism for redistributing nutrients and energy, and if the densities observed over southern United Kingdom are extrapolated to the airspace above all continental landmasses, high-altitude diurnal insect migration represents the most important annual animal movement in terrestrial ecosystems, comparable to the most significant oceanic migrations (21). Given the worrying declines in many migrants (8), developing global surveillance techniques (6) for long-term observation and prediction of the impacts of mass aerial migrations at such macrosystem scales (22) should be a priority for ecologists.

#### REFERENCES AND NOTES

- R. A. Holland, M. Wikelski, D. S. Wilcove, *Science* **313**, 794–796 (2006).
- S. Hahn, S. Bauer, S. Liechti, *Oikos* **118**, 624–626 (2009).
- J. W. Chapman *et al.*, *Science* **327**, 682–685 (2010).
- J. W. Chapman *et al.*, *Proc. Natl. Acad. Sci. U.S.A.* **109**, 14924–14929 (2012).
- J. W. Chapman, D. R. Reynolds, K. Wilson, *Ecol. Lett.* **18**, 287–302 (2015).
- R. Kays, M. C. Crofoot, W. Jetz, M. Wikelski, *Science* **348**, aaa2478 (2015).
- E. Warrant *et al.*, *Front. Behav. Neurosci.* **10**, 77 (2016).
- D. S. Wilcove, M. Wikelski, *PLOS Biol.* **6**, e188 (2008).
- K. Green, *Austral. Ecol.* **36**, 25–34 (2011).
- S. Bauer, B. J. Hoye, *Science* **344**, 1242552 (2014).
- J. S. Landry, L. Parrott, *Ecosphere* **7**, e01265 (2016).
- H. Mouritsen, D. Heyers, O. Güntürkün, *Annu. Rev. Physiol.* **78**, 133–154 (2016).
- T. Alerstam *et al.*, *Proc. Biol. Sci.* **278**, 3074–3080 (2011).
- V. A. Drake, D. R. Reynolds, *Radar Entomology: Observing Insect Flight and Migration* (CABI, Wallingford, UK, 2012).
- Supplementary materials and methods are available on Science Online.
- J. W. Chapman, D. R. Reynolds, A. D. Smith, E. T. Smith, I. P. Woivod, *Bull. Entomol. Res.* **94**, 123–136 (2004).
- C. Stefanescu *et al.*, *Ecography* **36**, 474–486 (2013).
- J. W. Chapman *et al.*, *Curr. Biol.* **18**, 514–518 (2008).
- J. W. Chapman *et al.*, *Curr. Biol.* **25**, R751–R752 (2015).
- J. J. Elser *et al.*, *Nature* **408**, 578–580 (2000).
- O. Varpe, O. Fiksen, A. Slotte, *Oecologia* **146**, 443–451 (2005).

22. J. F. Kelly, K. G. Horton, *Glob. Ecol. Biogeogr.* **25**, 1159–1165 (2016).

#### ACKNOWLEDGMENTS

G.H.'s visiting scholarship was funded by the China Scholarship Council. We acknowledge the support provided by COST—European Cooperation in Science and Technology through the Action ES1305 “ENRAM.” The project was supported by UK Biotechnology and

Biological Sciences Research Council grant BB/J004286/1 to J.W.C. Data are available at Dryad at <http://dx.doi.org/10.5061/dryad.6kt29>.

#### SUPPLEMENTARY MATERIALS

[www.sciencemag.org/content/354/6319/1584/suppl/DC1](http://www.sciencemag.org/content/354/6319/1584/suppl/DC1)  
Materials and Methods  
Figs. S1 to S8

Tables S1 to S8  
References (23–49)

27 June 2016; accepted 22 November 2016  
10.1126/science.aah4379

## BRAIN RESEARCH

# Active cortical dendrites modulate perception

Naoya Takahashi,<sup>1</sup> Thomas G. Oertner,<sup>2</sup> Peter Hegemann,<sup>3</sup> Matthew E. Larkum<sup>1\*</sup>

There is as yet no consensus concerning the neural basis of perception and how it operates at a mechanistic level. We found that  $\text{Ca}^{2+}$  activity in the apical dendrites of a subset of layer 5 (L5) pyramidal neurons in primary somatosensory cortex (S1) in mice is correlated with the threshold for perceptual detection of whisker deflections. Manipulating the activity of apical dendrites shifted the perceptual threshold, demonstrating that an active dendritic mechanism is causally linked to perceptual detection.

Recent studies in awake rodents indicate that dendritic  $\text{Ca}^{2+}$  activity in L5 cortical pyramidal neurons is elevated during cognitive processes (1–4). These studies are in line with the proposal that the  $\text{Ca}^{2+}$  electrogenic properties of the apical dendrites of pyramidal neurons (5, 6) amplify the effects of feedback inputs [apical amplification (7)] to superficial cortical layers (8, 9). There is evidence for the crucial role of feedback to primary sensory regions in perceptual processes (11, 12), but it still remains to be demonstrated experimentally that perception depends on a dendritic mechanism. We reasoned that the decisiveness of this mechanism could be tested by examining dendritic  $\text{Ca}^{2+}$  activity around the perceptual threshold that corresponds to the transition from subliminal to liminal perception in humans (13). The apical amplification hypothesis predicts that dendritic  $\text{Ca}^{2+}$  activity in a subset of neurons correlates to this transition, leading to the detection of stimuli (Fig. 1A). To test this experimentally, we used a whisker-based tactile detection task in mice (10) combined with two-photon  $\text{Ca}^{2+}$  imaging of pyramidal apical dendrites in S1. Additionally, we investigated the causal relationship between dendritic  $\text{Ca}^{2+}$  and perceptual detection by testing whether manipulating dendritic  $\text{Ca}^{2+}$  currents alters detection.

Animals were first trained to report whisker deflections by licking to obtain water rewards (Fig. 1, B and C). The C2 whisker was selectively stimulated using a magnetic coil (fig. S1). The mice learned the task (>80% correct “hit” re-

sponses), with low false alarm rates (i.e., the licking rate at zero stimulus intensity), within 2 weeks, at which point we determined the psychometric function for whisker stimulation by using a range of intensities above and below the perceptual detection threshold (Fig. 1D). The perceptual detection threshold for individual animals was determined by fitting the psychometric function with a sigmoid function (14) (Fig. 1E). The behavioral thresholds remained at the same level across sessions over days (Fig. 1F). The delay between the whisker deflection and an animal’s reaction (first lick) in “hit” trials was shorter in the trials of salient stimuli than in threshold stimuli (Fig. 1G).

We simultaneously performed fast-scanning two-photon  $\text{Ca}^{2+}$  imaging from apical dendrites of L5 neurons in the C2 barrel column in primary somatosensory cortex (S1) (Fig. 1H). In each field of view (175 by 175  $\mu\text{m}$ ),  $98.1 \pm 17.8$  apical dendrites were identified at 200 to 300  $\mu\text{m}$  below the pia (mean  $\pm$  SD,  $n = 8$  sessions from 8 mice). During the behavior, large  $\text{Ca}^{2+}$  transients were observed in some apical dendrites after whisker deflections (Fig. 1I). To investigate the relationship between dendritic activity and perceptual behavior of the animal,  $\text{Ca}^{2+}$  responses were determined for seven different stimulus intensities around the behavioral threshold (Fig. 1I, vertical columns). We compared the activity in “lick” trials (Fig. 1I, lower rows) to “no-lick” trials (upper rows) and averaged the responses over all trials (bottom traces).

How does dendritic  $\text{Ca}^{2+}$  relate to behavior for this whisker detection task? To examine this, we plotted the dendritic  $\text{Ca}^{2+}$  response as a function of stimulus intensity—i.e., the neurometric function—versus detection probability as a function of stimulus intensity—i.e., the psychometric function (Fig. 2A, right). In some cases, the increase in dendritic  $\text{Ca}^{2+}$  closely followed the behavioral performance of the animal (Fig. 2A).

Interestingly, in a smaller fraction of cases, we found the opposite: dendritic  $\text{Ca}^{2+}$  anticorrelated with stimulus strength (Fig. 2A), which may be indicative of a parallel coding scheme such as predictive coding (15). The correlation of dendritic  $\text{Ca}^{2+}$  to behavior was quantified using a similarity index (SI) (16) and compared to chance level by shuffling the stimulus intensities of the original data (Fig. 2B). In 34% (267 of 785) of cases, the SIs deviated from chance. The fraction of dendrites responding to salient whisker deflections was greater in mice engaged in the task than naïve (untrained) mice (fig. S2).

We also investigated the discriminability of dendritic  $\text{Ca}^{2+}$  by evaluating the behavioral outcome (hit or miss) versus the  $\text{Ca}^{2+}$  response near the threshold for behavior—i.e., the discrimination index (DI) based on a receiver operating characteristic (ROC) analysis (17) (Fig. 2C) (also see methods in the supplementary materials). In 22% (173 of 785) of dendrites, the dendritic  $\text{Ca}^{2+}$  near threshold alone could be used to predict the behavior with prolonged increases in  $\text{Ca}^{2+}$  signals in “lick” trials, but not in “no-lick” trials (Fig. 2D, \*DI > 0,  $P < 0.05$ ; and Fig. 2E, left). Again, in some neurons (68 of 785), the behavior was predicted by a decrease in dendritic  $\text{Ca}^{2+}$  (Fig. 2D, \*DI < 0,  $P < 0.05$ ; and Fig. 2E, right). In another group of neurons with high SIs and low DIs, evoked  $\text{Ca}^{2+}$  signals increased with increasing amplitudes of whisker deflection but were independent of behavioral outcome, suggesting that these neurons coded for information orthogonal to perceptual detection (Fig. 2E, middle). We characterized the temporal and spatial features of perception-relevant dendrites (DI’s  $P < 0.05$ ). The timing of the dendritic  $\text{Ca}^{2+}$  increases for high stimulus strengths was faster than that for near-threshold stimuli, and the dendritic  $\text{Ca}^{2+}$  mostly preceded the behavior (Fig. 2F and fig. S3). We found a small but significant relationship between the physical location of the dendrites and their DI (Fig. 2, G and H).

Activation of dendritic  $\text{Ca}^{2+}$  channels results in enhanced firing of individual L5 pyramidal neurons in vivo (18). We monitored the firing activity of L5 neurons while the animal performed the whisker detection task (Fig. 3A). The results of 40 cells recorded from L5 (depth, 577.8 to 774.0  $\mu\text{m}$  below the pia) in behaving animals were pooled. Mean firing rates were  $11.1 \pm 14.2$  Hz, ranging from 0.68 to 63.1 Hz (mean  $\pm$  SD,  $n = 40$  cells from 10 mice). In a fraction of neurons, perceived whisker stimuli increased firing activity, resulting in positive correlations between neurometric and psychometric functions (Fig. 3B). As seen in dendritic  $\text{Ca}^{2+}$  activity, we also observed some cells for which the firing activity

<sup>1</sup>Institute for Biology, Neuronal Plasticity, Humboldt Universität zu Berlin, D-10117, Berlin, Germany. <sup>2</sup>Institute for Synaptic Physiology, University Medical Center Hamburg-Eppendorf, D-20251, Hamburg, Germany. <sup>3</sup>Institute for Biology, Experimental Biophysics, Humboldt Universität zu Berlin, D-10115, Berlin, Germany.

\*Corresponding author. Email: [matthew.larkum@hu-berlin.de](mailto:matthew.larkum@hu-berlin.de)

EXTENDED PDF FORMAT  
SPONSORED BY



### Mass seasonal bioflows of high-flying insect migrants

Gao Hu, Ka S. Lim, Nir Horvitz, Suzanne J. Clark, Don R. Reynolds, Nir Sapir and Jason W. Chapman (December 22, 2016)  
*Science* **354** (6319), 1584-1587. [doi: 10.1126/science.aah4379]

#### Editor's Summary

#### Mass movement of "invisibles"

We know a lot about vertebrate migrations globally. However, the majority of animals that live on this planet are invertebrates, and we know very little about their movements. Hu *et al.* monitored the migration of large and small insects over the southern United Kingdom for a decade. They found that more than a trillion insects move across this region annually. The movement of such a large biomass has considerable impacts on the ecosystems between which the insects migrate.

*Science*, this issue p. 1584

---

This copy is for your personal, non-commercial use only.

---

- Article Tools** Visit the online version of this article to access the personalization and article tools:  
<http://science.sciencemag.org/content/354/6319/1584>
- Permissions** Obtain information about reproducing this article:  
<http://www.sciencemag.org/about/permissions.dtl>

*Science* (print ISSN 0036-8075; online ISSN 1095-9203) is published weekly, except the last week in December, by the American Association for the Advancement of Science, 1200 New York Avenue NW, Washington, DC 20005. Copyright 2016 by the American Association for the Advancement of Science; all rights reserved. The title *Science* is a registered trademark of AAAS.